Ultra-Thin a-Ge:H Solar Cell with Switchable Absorption Enhancement: Towards Smart Photovoltaic Windows

This is the accepted proof of the Confernece Proceeding of the 2020 47th IEEE Photovoltaic Specialists Conference (PVSC).

https://doi.org/10.1109/PVSC45281.2020.9300671

Cite as:

M. Götz, K. Gehrke, H. Meddeb, M. Vehse and C. Agert, "Ultra-Thin a-Ge:H Solar Cell with Switchable Absorption Enhancement: Towards Smart Photovoltaic Windows," *2020 47th IEEE Photovoltaic Specialists Conference (PVSC)*, 2020, pp. 1114-1118, doi: 10.1109/PVSC45281.2020.9300671

The copyright of the Work is with The Institute of Electrical and Electronics Engineers (IEEE)

© IEEE 2021

Ultra-Thin a-Ge:H Solar Cell with Switchable Absorption Enhancement: Towards Smart Photovoltaic Windows

Maximilian Götz
DLR Institute of Networked Energy Systems
Oldenburg, Germany
maximilian.goetz@dlr.de

Kai Gehrke
DLR Institute of Networked Energy Systems
Oldenburg, Germany
kai.gehrke@dlr.de

Hosni Meddeb
DLR Institute of Networked Energy Systems
Oldenburg, Germany
hosni.meddeb@dlr.de

Martin Vehse
DLR Institute of Networked Energy Systems
Oldenburg, Germany
martin.vehse@dlr.de

Carsten Agert
DLR Institute of Networked Energy Systems
Oldenburg, Germany
carsten.agert@dlr.de

***Abstract*— Realizing a window with power generation on-demand and light management at the same time is one of the most intriguing challenges of the building-integrated photovoltaic community. We present an approach for a switchable solar window that enables a reversible transition from a light absorption state, which results in a photo-generated current, to a semi-transparent state. The device is based on an ultra-thin amorphous germanium layer, arranged in an optical cavity for broadband light absorption. The applicability of our device is tested by modeling the switching behavior in a realistic scenario.**

Keywords— window-integrated PV, switchable PV, thin film solar cells, cavity enhanced absorption

I. Introduction

In metropolitan areas and megacities around the globe, a large part of the facades are built with glass. Large windows in particular are installed in modern office buildings, which require a modern shading system for effective light and heat management. The development of smart windows that enable dynamic daylight control in buildings has attracted great interest in recent years [1-6]. It was already shown, that switchable windows can effectively provide significant cooling savings for buildings [3]. Furthermore, the combination of such switchable windows with semi-transparent thin-film photovoltaic modules is promising for the coupling of power generation with effective light management [7]. The integration of solar cell devices into the window façade should enable both the harvesting of illumination for electricity generation as well as light transmission for clear visibility. For this purpose, the switchable photovoltaic window is considered as promising concept since it provides the capability of mutual transition from a solar cell mode in opaque state to window mode in transparent state. In this contribution, we present the concept and the realization of a switchable photovoltaic window based on the light trapping modulation in an optical cavity. Furthermore, we demonstrate based on a geometrical model of the direct solar irradiance on the windows, that a power output of up to 200 Wh/day/m² can be achieved in a real switching scenario.

II. Device Structure

For the realization of a smart photovoltaic window, a device enabling reversible switching from a transparent state to an absorbing photovoltaic state is required.

The switchable absorption is established using a simple layer configuration as shown in Figure 1. An absorptive medium with high extinction coefficient (n~k) and sub-wavelength thickness is positioned between a transparent dielectric and a metallic medium. By changing the thickness of the absorber layer and the reflection coefficients at the interfaces, the phase change of the light can be adjusted to match resonance conditions. This leads to enhanced absorption inside the layer stack. The absorption enhancement is switched “off”, when the resonance conditions inside the cavity are disturbed. This was realized using 25 nm thick Mg as a rear metal layer[8]. Mg drastically changes its optical

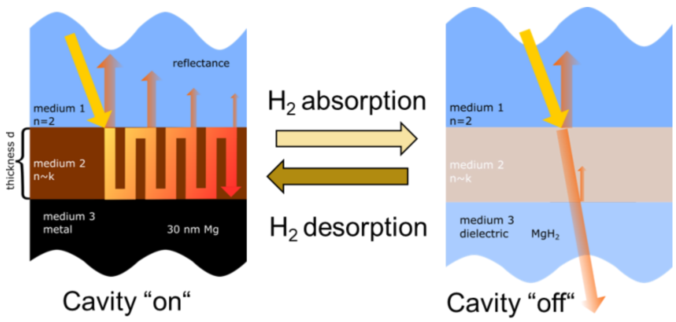

Fig. 1. Illustration of the layer stack for switchable absorption enhancement

properties, when exposed to H_2. It switches from a metallic to a dielectric transparent state by incorporating hydrogen atoms, turning into magnesium hydride (MgH_2)[9]. This change of optical properties was used to switch the absorption enhancement "off" and make the device transparent. The switching process is initiated by exposing the device to 5 % H_2 in N_2 at atmospheric pressure and requires less than 15 minutes. The gas mixture is non-explosive and non-flammable. The hydrogen desorption process takes place at ambient air and requires another 15 minutes.

Figure 2 presents the solar cell structure including a 5 nm thick layer of a-Ge:H as nano-absorber embedded between p- and n-doped a-Si layers. A ZnO:Al transparent and conductive layer is used as front contact, while the switchable Mg layer is used as back contact. A Pd capping layer is added to prevent the layers from oxidation and acts as catalyst for hydrogen absorption [10]. The front ZnO:Al layer has a thickness of 400 nm to improve the charge carrier extraction and reduce ohmic losses. This adds additional interference peaks to the transmission and absorption spectra. To avoid the interference fringes in the simulation only 80 nm of ZnO:Al are used for modeling. The ZnO:Al layer was deposited by a magnetron sputtering process. The Si and Ge layers are fabricated by plasma enhanced chemical vapor deposition. Mg and Pd layers are deposited via electron beam evaporation.

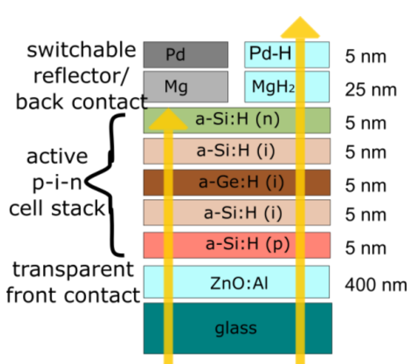

Fig. 2. Illustration of the layers stack of a switchable photovoltaic window

II. Results and Discussion

The main aspects to be considered for transparent and switchable photovoltaics are the optical appearance, the charge carrier generation and the performance in different switching scenarios. Here we focus on the photocurrent generation, as well as the application case of switchable windows in a building facade. First we show the results from 1D transfer matrix simulations followed by measurements of real devices. The layer stack displayed in Fig. 2 is modeled, using refractive index data deduced from transmission and reflection measurements of single layers. The layer thickness of the ZnO:Al layer is assumed to be 80 nm, to reduce additional interference effects. Figure 3 (a) presents the simulated transmission spectra of the switchable photovoltaic window in two states: With a metallic Mg rear contact, the cavity is switched "on". After hydrogen absorption the resonator is switched "off". The transmission increases from $T \approx 5$ % to $T \approx 18$ % at the spectral position of 500 nm by switching the resonator off. For longer wavelengths the difference between both states increases. By switching the Mg/Pd layer, not only the transparency is changed, but also the cavity is switched "off". This can be seen in the simulated external quantum efficiency (EQE) of the a-Ge:H layer by assuming a conversion efficiency of 100 %, presented in Figure 2 (b). The simulated EQE is plotted for the reference cell with 300 nm Mg back contact (cavity "on", reference) and a cell with Mg/Pd back contact in hydrogenated (cavity "off") and metallic state (cavity "on"). The simulation does not take into account the electrical contact losses and recombination through defects. The solar cell with Mg / Pd rear contact in cavity "on" state reaches similar EQE level as the reference cell with 300 nm Mg back reflector. Small deviations at wavelengths between 600 - 800 nm can be explained by the remaining light transmission in the thin Mg/Pd layers. After hydrogenation, the photocurrent generation decreases significantly, due to the fact that the Mg layer no longer confines the electric field in the cavity[11].

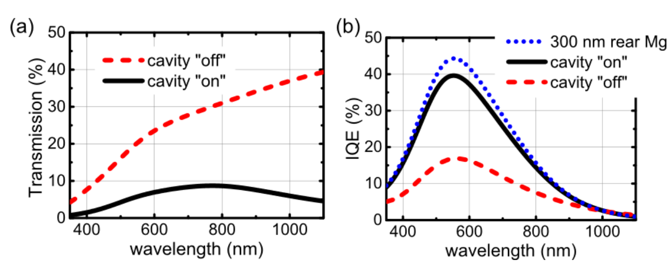

Fig. 3. Simulation of switchable solar c ell: Simulated transmission (a) and simulated quantum efficiency (b) in "on" and "off" state.

The vanishing of the optical resonance effect is correlated with the switching of the reflector into the transparent state. The estimated photocurrent can be calculated from the simulation by multiplication of the spectra with the photon flux of the AM1.5 solar spectrum and their integration over the whole spectral range. This simulation results in an estimated photocurrent of J_{EQE}(300 nm Mg) = 9.85 mA/cm²,

J_{EQE}(“on”) = 8.95 mA/cm² and J_{EQE}(“off”) = 4.42 mA/cm², respectively.

After the modeling study of the switchable layers stack, the fabrication and the optoelectronic characterization of solar cell devices are performed. Figure 4 presents the measured JV and external quantum efficiency curves of the solar cell with thick (300 nm) Mg rear mirror to improve the electrical contacts. The cell reaches an efficiency of 1.7 % with a fill factor (FF) of 41.2 %, an open circuit voltage (V_{OC}) of 467 mV and a short circuit current density (J_{SC}) of 7.83 mA/cm².

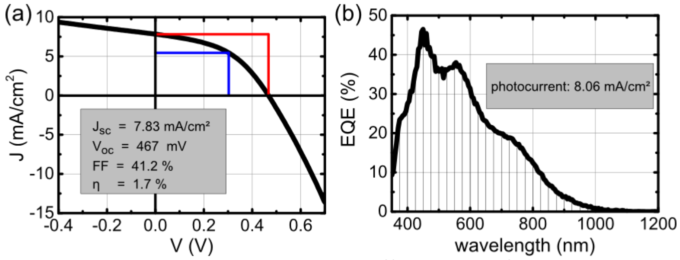

Fig. 4. JV curve (a) and external quantum efficiency (b) of the same cell with 300 nm Mg rear contact

The EQE reaches a maximum value of 46 % at a wavelength of 445 nm. The overall EQE corresponds to a photocurrent of J_{EQE}=8.06 mA/cm², which is 1.79 mA/cm² less than predicted from simulation. The difference can be explained by extra parasitic absorption due to the thicker ZnO:Al of the fabricated device (400 nm) compared to the ZnO:Al layer considered in simulation (80 nm), as well as additional electrical losses, due to recombination.

Fig. 5 (a) presents the measured spectral transmission of the switchable solar cell with a 30 nm Mg and 5 nm Pd rear contact in cavity “on” and “off” state. In the “off” state, a transparency of up to 30 % is reached. The additional interference patterns in the spectra originate from the thick AZO front contact, which is in contrast to the 80 nm thick front contact in the simulation. It can be clearly seen, that the transmission changes drastically between both states. Figure 5 (b) shows an image of a 10x10 cm² device with 16 working solar cells with Mg Pd rear contacts. The areas without metallic rear contact are semi-transparent. The remaining brownish color is caused by the a-Ge and a-Si layers. This color can also be expected in the cavity off-state of the solar cell.

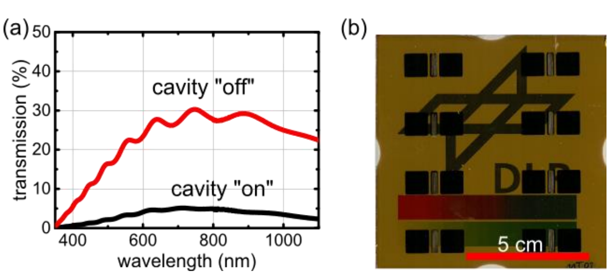

Fig. 5. Measured transmission (a) in transparent (red) and opaque (black) mode and image of a 10x10 cm² device with 16 cells (b).

Our experimental and simulation results demonstrate the feasibility of a switchable photovoltaic window based on gasochromic Mg/Pd back reflector. The solar cell is able to reach an EQE of 48 % in the cavity “on” state (Fig. 4 (b)) with only 5 nm a-Ge:H absorber layer. The moderate efficiency of 1.7 % (Fig. 4 (a)) might be sufficient to improve the ecological footprint of buildings with large glass façades. The increase in transparency by six folds (Fig. 5) after hydrogen absorption also demonstrates that the device can be used as a switchable window for natural light management.

Further improvements and considerations are required for the specific implementation of the previously demonstrated device technology in real buildings. Nevertheless, the estimation of the power generation capability of such switchable photovoltaic window is desired. Therefore, we created a model which tracks the direct radiation onto a switchable window with 5% efficiency installed vertically in the building façade. Previous publications have already shown, that 5% efficiency can be reached using this technology [11]. For the model, we considered windows facing in four different cardinal directions: south (S), south-west (SW), west (W) and north (N). The windows are - unlike normal solar cells - not positioned for best radiation income, but vertically in the building facade. Figure 6 depicts the angle between solar window and sun for a south facing window, for three different situations. Only the case in Figure 6 (a) leads to power generation by photo-conversion of the direct irradiation from sun light. Figure 6 (b) shows the scenario in which the sun is behind the solar cell and Figure 6 (c) the scenario after sunset. The position of the sun, which is determined by the latitude of the location on earth, becomes a limiting factor for the generated power. Higher sun altitude is less beneficial for the direct irradiation shining over the window surface. The elevation and azimuth of the sun also depend on the season. It is unfavorable for the power generation of the solar window, when the sun reaches elevations of 90°, resulting in drastically reduced time of exposure to direct irradiation. In both cases only diffuse radiation is absorbed by the solar cell.

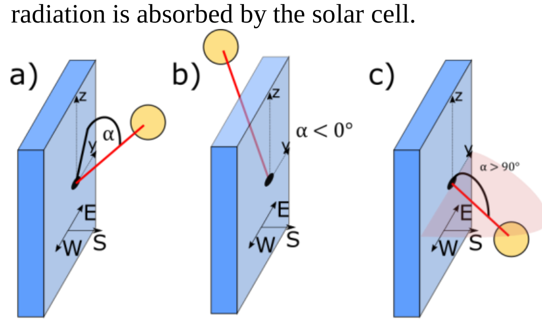

Fig. 6. Schematic drawing of geometry between sun and south facing window for different positions of the sun: (a) Direct radiation can be absorbed by the photovoltaic window. (b) The sun is behind the solar cell in and no direct radiation shines on the cell. (c) The sun is below the horizon

The altitude and azimuth of the sun are computed using the python package *pysolar* (v 0.6) [12]. Starting with sunrise, the position of the sun is evaluated in 500 equally spaced steps of time between sunrise and sunset. The angle α between sun and solar window is calculated by converting the sun's position to Cartesian coordinates and using of following equation with the standard scalar product:

$$\cos(\alpha) = \frac{\vec{v}_{Sun} \cdot \vec{u}_{window}}{|\vec{v}_{Sun}||\vec{u}_{window}|}$$

Here, $\vec{v}_{Sun}$ indicates the position of the sun and $\vec{u}_{window}$ describes the surface normal of the solar cell. This term is multiplied with the atmospheric corrected direct radiation to get the power output of a solar window. The location of the solar window for the current model is Oldenburg in Germany at 53.15° N and 8.17° E.

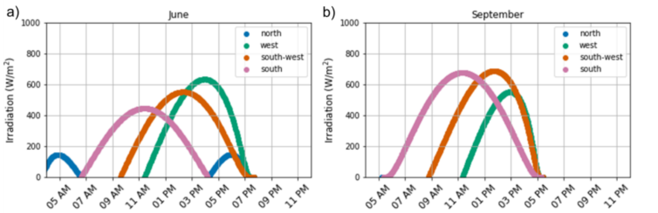

Fig. 7. Simulation of direct sun light irradiation on a S, SW, W and N facing window on June 15th (a) and September 15th (b). The x axis shows the time in coordinated universal time.

Figure 7 (a) and (b) present the direct radiation incident onto windows facing in the directions S, SW, W and N in June and September, respectively. In June, the south facing window only receives little direct radiation from the sun. The sun rises behind the window in the north-eastern direction and never reaches a preferable angle of incidence to the window area before the sunset in the west. The direct radiation illuminating the W and SW facing window is higher during summer, because in both positions the photovoltaic window can absorb light from a lower angle, when the sun sets in the west. In fall, when the elevation of the sun is lower in the northern hemisphere, the exposure to radiation for the S facing window is increased. These observations lead to the results displayed in Figure 8 (a) and (b). Here, the power output of a switchable photovoltaic window with 5% efficiency in "on" and zero percent efficiency in "off" mode is shown. If the cell would be kept in "on" mode for a complete year, a south facing module would generate up to 250 Wh/m²/day in spring and fall, only from direct radiation. A west facing photovoltaic window would still allow to generate more than 150 Wh/m²/day in the summer months.

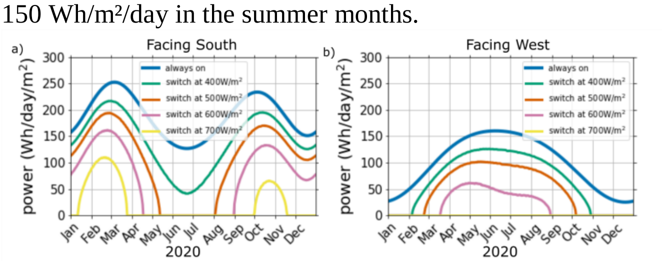

Fig. 8. Simulation of the power output of a solar window with 5 % efficiency facing (a) south or (b) west. The model turns the window into solar cell mode after the direct irradiation exceeds the respective threshold value.

In order to analyze the performance of photovoltaic windows, the switching model scenarios are defined. There are several different approaches for the simulation of the switching behavior [3]. The most important aspects to be considered are the location of the window, its orientation and the times it is switched into transparent or solar cell mode. A threshold model can set a certain level of direct irradiation to trigger the switching process. Hereby, the window would be transparent for irradiance below the threshold value and in photovoltaic state above the threshold. The best case scenario which we used in our model does not include weather data like clouds, shadow or snow. Figure 8 (a) and (b) presents graphs for switching thresholds of 400, 500, 600 and 700 W/m² of direct irradiation on to the windows. This corresponds to the direct radiation transmitted through the window and entering the interior of the building. The model shows, that the power output of an S facing window would be drastically reduced during the time from April to September. The direct radiation does almost never meet the condition of exceeding the threshold value and the window would be kept in transparent mode. The expected decrease of power output can also be seen for the W facing window. During winter months, when the daylight time is shorter, the usage of these photovoltaic windows would be limited. However, in the summer months, the W facing photovoltaic window would enable the generation of significant power outcome, especially when switched "on" in the afternoon. This shows that a combination of switchable photovoltaic windows facing in different directions could support the electricity generation during the complete day as well as over the whole year.

III. Conclusion & Outlook

This study reports on a switchable solar cell based on a gasochromic Mg/Pd mirror applied as a back reflector of an ultrathin a-Ge:H based resonant cavity enhanced solar cell. The thin Mg/Pd layers allow the device to switch between a transparent and an absorptive state, corresponding to "off" and "on" modes of the optical cavity. While working as fully functional solar cell in the cavity "on" state, the device turns into a transparent window mode after the absorption of hydrogen in the Mg/Pd layers.

The presented device is a first step towards the realization of large scale switchable photovoltaic windows. The optoelectronic results show that using ultra-thin a-Ge:H absorber layers is a promising way to reach high transparency while maintaining color neutrality. The simulation of the power generation in different scenarios shows, that using a 5 % efficiency switchable solar cell, a power output of up to 250 Wh/m²/day could be realized by using only direct sunlight. The accuracy of the presented simulations will be further increased by using real weather data and including also diffuse light. The successful demonstration of the promising potential of the switchable solar cells in our work can pave the route for further valuable contribution to the existing BIPV concepts.

ACKNOWLEDGMENT

The authors thank U. Banik, C. Lattyak, N. Osterthun and D. Berends for fruitful discussion and supporting this publication.

References

[1] P. Lemarchand, J. Doran, and B. Norton, "Smart switchable technologies for glazing and photovoltaic applications," *Energy Procedia,* vol. 57, pp. 1878-1887, 2014.

[2] C. G. Granqvist, "Electrochromics and Thermochromics: Towards a New Paradigm for Energy Efficient Buildings," *Materials Today: Proceedings,* vol. 3, pp. S2-S11, 2016.

[3] J.-M. Dussault and L. Gosselin, "Office buildings with electrochromic windows: A sensitivity analysis of design parameters on energy performance, and thermal and visual comfort," *Energy and Buildings,* vol. 153, pp. 50-62, 2017.

[4] M. Yao, T. Li, Y. Long, P. Shen, G. Wang, C. Li*, et al.*, "Color and transparency-switchable semitransparent polymer solar cells towards smart windows," *Science Bulletin,* vol. 65, pp. 217-224, 2020.

[5] X. H. Li, C. Liu, S. P. Feng, and N. X. Fang, "Broadband Light Management with Thermochromic Hydrogel Microparticles for Smart Windows," *Joule,* vol. 3, pp. 290-302, 2019.

[6] Y. Ke, J. Chen, G. Lin, S. Wang, Y. Zhou, J. Yin*, et al.*, "Smart Windows: Electro‐, Thermo‐, Mechano‐, Photochromics, and Beyond," *Advanced Energy Materials,* vol. 9, p. 1902066, 2019.

[7] H. K. Kwon, K. T. Lee, K. Hur, S. H. Moon, M. M. Quasim, T. D. Wilkinson*, et al.*, "Optically Switchable Smart Windows with Integrated Photovoltaic Devices," *Advanced Energy Materials,* vol. 5, p. 1401347, Feb 4 2015.

[8] M. Götz, M. Lengert, N. Osterthun, K. Gehrke, M. Vehse, and C. Agert, "Switchable Photocurrent Generation in an Ultrathin Resonant Cavity Solar Cell," *ACS Photonics,* vol. 7, pp. 1022-1029, Apr 15 2020.

[9] X. Duan, R. Griessen, R. J. Wijngaarden, S. Kamin, and N. Liu, "Self-recording and manipulation of fast long-range hydrogen diffusion in quasifree magnesium," *Phys. Rev. Materials,* vol. 2, p. 85802, 2018.

[10] T. J. Richardson, J. L. Slack, R. D. Armitage, R. Kostecki, B. Farangis, and M. D. Rubin, "Switchable mirrors based on nickel-magnesium films," *Applied Physics Letters,* vol. 78, pp. 3047-3049, 2001.

[11] M. Götz, N. Osterthun, K. Gehrke, M. Vehse, and C. Agert, "Ultrathin Nano-Absorbers in Photovoltaics: Prospects and Innovative Applications," *Coatings,* vol. 10, p. 218, Mar 2020.

[12] B. Stafford. (2014, 02.06.2020). *Pysolar Documentation*. Available: https://pysolar.readthedocs.io/en/latest/#